POLITECNICO DI TORINO
Repository ISTITUZIONALE

CO2 abatement and CH4 recovery at vehicle exhausts: Comparison and characterization of Ru powder and pellet catalysts

Original
CO2 abatement and CH4 recovery at vehicle exhausts: Comparison and characterization of Ru powder and pellet catalysts / Murena, F., Esposito, S., Deorsola, F.A., Galletti, C., Prati, M.V.. - In: INTERNATIONAL JOURNAL OF HYDROGEN ENERGY. - ISSN 0360-3199. - 45:15(2020), pp. 8640-8648. [10.1016/j.ijhydene.2020.01.120]

Availability:
This version is available at: 11583/2801706 since: 2020-03-24T09:04:43Z

Publisher:
Elsevier Ltd

Published
DOI:10.1016/j.ijhydene.2020.01.120

Terms of use:

This article is made available under terms and conditions as specified in the corresponding bibliographic description in the repository

Publisher copyright

(Article begins on next page)

15 October 2026

CO_2 abatement and CH_4 recovery at vehicle exhausts: comparison and characterization of Ru powder and pellet catalysts

F. Murena[1*], S. Esposito[2*], F.A. Deorsola[2], C. Galletti[2] and M.V. Prati[3]

[1] Department of Chemical, Materials and Production Engineering - University of Naples "Federico II" – Italy

[2] Department of Applied Science and Technology and INSTM Unit of Torino – Politecnico, Corso Duca degli Abruzzi 24, 10129, Torino, Italy.

[3] Istituto Motori - National Council of Research - Naples - Italy

Corresponding authors: Fabio Murena: murena@unina.it; Serena Esposito: serena_esposito@polito.it

ABSTRACT

The catalytic conversion of CO_2 to CH_4 (Sabatier reaction) has been studied to develop an after-treatment process at vehicles exhausts. Three different formulations of Ru commercial catalysts, two in powder and one in pellets shape, were tested and characterised by means of X-ray powder diffraction, scanning electron microscopy (SEM-EDX), N_2 adsorption at -196 °C and temperature-programmed reduction (TPR).

Experimental results show a high CO_2 conversion (X_{CO2}=0.96 @ T=280 °C) for one powder catalyst formulation whereas the other one has maximum CO_2 conversion = 0.69. In both cases a high CH_4 selectivity is measured. High CO_2 conversion (X_{CO2}=0.92 @ T=300 °C) is obtained also with pellet catalysts but only at lower GHSV values. The different behaviour of the catalysts was ascribed to the different physicochemical properties and the key parameters for the application development of the process were identified. In particular, the possibility to use pellets or monolithic reactors, thus minimizing the pressure drops in the reactor, makes possible a commercial application in the treatment of vehicles exhausts.

Keywords: CO_2 remediation, methanation, Sabatier reaction, Ru catalysts, pellets, vehicles exhaust

1. INTRODUCTION

The reaction of CO_2 methanation, discovered in 1902 by Sabatier and Senderens [1], is attracting much interest because represents a promising solution to reduce the global warming effect due to anthropogenic emissions. Carbon dioxide has a relatively low Global-Warming Potential (GWP): 3.7 times less than methane, 180 times less than nitrous oxide and from 103 to 104 times less than fluorinated gases [2]. However, due to the high emission rates, CO_2 is the most important of greenhouse gases.

Main strategies to reduce CO_2 emissions are capture and storage (CCS) or conversion in organic reusable compounds, especially gaseous or liquid fuels in the so-called Power-To-Gas (P2G) or Power-To-Liquid (P2L) pathway [3]. CO_2 capture is realized mainly through absorption or adsorption [4,5].

Even though the most of studies are on absorption or adsorption, the conversion of CO_2 into organic reusable compounds [6,7] is a very challenging approach and fits to the principles of circular economy.

Several studies and reviews have focused on different aspects of the methanation reaction: development of catalysts, reaction performances and reactor design [8–17]. Kinetic studies have been reported by Falbo et al. [10] and Champon et al. [11], even coupled with system integration [18]. The CO_2 methanation is a possible end-of-pipe operation of several industrial processes: biomass combustion and gasification, biogas plants, power plants, cement kilns and other. The role of catalysis in boosting the CO_2 utilization has been deeply analysed by Aresta et al. [12].

Data from the European Commission indicate that the transport sector represents about 25% of Europe greenhouse gas emissions, with road transport acting as the largest emitter inside the sector (about 70% of the whole). Moreover, the trend of decreasing transport emissions is lower than in other sectors [19]. Inside the transportation sector, the four-wheels vehicle sector on its own is responsible for about 12% of total EU CO_2 emissions [20]. Therefore, if a significant reduction in overall CO_2 emissions must be achieved, it is necessary to find feasible processes also for the transport sector and specifically for the road transport sub-sector. On 17 April 2019, the European Parliament and the Council adopted Regulation (EU) 2019/631 setting new CO_2 emission standards for cars and vans. From 1 January 2020, an EU fleet-wide target of 95 g CO_2 km^{-1} for the average emissions of new passenger cars is set [20]. This means a fuel

consumption of around 4.1 L 100 km^{-1} of petrol or 3.6 L 100 km^{-1} of diesel. Moreover, from 1st January 2025 the CO_2 km^{-1} target will be reduced to 15% of the 2020 target and from 1st January 2030 it will be further reduced to 37.5% of the 2020 for new passenger cars. According to the European Parliament, manufacturers whose average emissions exceed the limits will have to pay an excess emissions premium. The application of methanation for CO_2 remediation at vehicle exhausts is a particularly intriguing but complex task. Very few papers deal with the application of methanation at vehicles exhaust. Murena et al. [21] report the results of some tests at the exhausts of two vehicles: a Parvisa Myspace 125 scooter and a FIAT Panda Natural Power. Performances in terms of conversion were generally very good and only slightly lower than those obtained with model gas mixtures. CO_2 conversion ranged from 0.75 to 0.97 with contact time of 1.26 s, corresponding to gas hourly space velocity GHSV, representing the ratio between the gas flow rate in standard condition and the volume of the active phase i.e. catalyst, of 402 mL h^{-1} g^{-1} at T = 300 °C and H_2/CH_4 stoichiometric ratio. In those tests [21], a commercial Ru 5 wt% on alumina powder with central size distribution between 45 and 75 μm was adopted as catalyst. Notwithstanding the substantial number of papers that ascertain the ruthenium activity in the reaction of CO_2 methanation [9,10,22–26], there is still lack of works illustrating the impact of structural, morphological and redox features of ruthenium-containing materials on their catalytic behavior in the case of CO_2 remediation at vehicle exhausts. Moreover, the use of powdered catalyst is not appropriate for practical applications at vehicles exhaust because of the high back pressure [27]. For this reason, a comparative study was carried out by using Ru supported on Al_2O_3 catalyst in the powder and pellet shape. The catalysts were tested in different operating condition (P = 1 atm; temperature in the range 200 – 350 °C; GHSV = 0.65 – 2 L $h^{-1}g^{-1}$ and H_2/CO_2 ratio = 4) and fully characterized by complementary techniques.

2. MATERIAL AND METHODS

The catalysts adopted were: Ruthenium 5 wt% on alumina, powder, reduced dry, 439916; Ruthenium 5 wt% on alumina, powder, Degussa Type, 381152; Ruthenium on alumina extent of labelling: 0.5 wt%, pellets, 3.2 mm, 206199. All catalysts were supplied by Aldrich. Catalysts were used as received without

any activation pre-treatment by reduction with hydrogen. All catalysts were characterized by X-ray powder diffraction (XRPD) on a Philips X'Pert diffractometer equipped with a Cu K_α radiation (2θ range = 10° - 80°; step = 0.02° 2θ; time per step = 1 s). Phase identification was performed by referring to the JCPDS PDF-2 Release 2002 database.

N_2 adsorption/desorption isotherms at -196 °C were determined on ca. 100 mg sample previously outgassed at 250 °C for 4 h to remove atmospheric contaminants (Quantachrome Autosorb 1 instrument). Specific surface area (S_{BET}) was calculated according to the BET (Brunauer-Emmett-Teller) method. The pore size distribution was calculated by applying the Non-Local Density Functional Theory (NL-DFT) method to isotherms adsorption branches.

TPR measurements were carried out on a TPD/R/O 1100 instrument (ThermoQuest) equipped with thermal conductivity detector (TCD) by using a 5 vol.% H_2/Ar mixture (Q = 20 cm^3 min^{-1}) with a heating rate of 10 °C min^{-1} up to 600 °C. In a typical experiment, ca. 100 mg sample was loaded in a quartz down-flow cell with a K-type thermocouple placed in close contact with the sample to measure the temperature. Field Emission Scanning Electron Microscopy (FESEM) was performed on a Zeiss Merlin microscope equipped with an EDS GEMINI II column. The observation and analysis of the catalyst in the pellet form was carried out on the cross-section fracture surface.

All catalytic experimental runs were carried out using a model gas mixture with CO_2 concentration at 9.5% volume in N_2. A comparison of the model mixture composition with average real vehicle exhaust is reported in Table 1. Comparison of previous results obtained with the model gas mixture (Table 1) and real vehicles exhaust coming from spark-ignited engines showed a good correlation [21]. For this reason, we can exclude a negative effect of the presence of O_2 on catalyst performances at least when spark ignition engines as those tested in [21] are considered. The experimental apparatus consisted of: i) three gas inlet lines (N_2/CO_2 mixture, pure H_2 and N_2 for cooling and washing operations) where mass flow rate was measured and controlled using mass flowmeters supplied by OMEGA srl: FLDN3503G for the N_2/CO_2 mixture and FLDH3305G for H_2; ii) a vertical cylindrical glass reactor (0.8 cm of internal diameter and 40 cm length) assembled in an oven with electrical heating and temperature controlled by

three thermocouples. The catalyst was loaded in the middle zone of the reactor to guarantee a homogeneous temperature; iii) a gas chromatograph (HP 5890) equipped with a Supelco-CARBOXEN 1006 PLOT column and a TCD detector to measure the gas concentrations in the flow leaving the reactor. More details on the experimental apparatus may be found in Murena et al. [21].

All runs were carried out at constant pressure (P = 1 atm) and constant H_2/CO_2 ratio equal to 4. The temperature levels tested were in the range 200-350 °C in isothermal conditions. The mass of catalyst loaded was varied from 1 g to 3 g to verify the effect of contact time on the reactive process. The total gas hourly space velocity (GHSV) is reported @ STP (T = 20 °C and P = 1atm) as litre of total inlet flow gas per hour and per gram of catalyst. The CO_2 volume percentage in the CO_2/N_2 mixture was 9.5%, a value similar to that measured at vehicles exhaust. Experimental runs were replicated to verify data accuracy and reproducibility.

The catalytic performance was evaluated by means of CO_2 conversion (X_{CO2}) and CH_4 yield (Y_{CH4}), defined as reported in Eq. 1 and 2. Standard deviation for X_{CO2} was also calculated.

$$X_{CO2}=\frac{CO_{2\,IN}-CO_{2\,OUT}}{CO_{2\,IN}} \quad (1)$$

$$Y_{CH4}=\frac{CH_{4\,OUT}}{CO_{2\,IN}} \quad (2)$$

Table 1 Average volume percentage of main components of real vehicle exhaust gas compared with the model gas composition used

	N_2	CO_2	CO	O_2	H_2O
gasoline motor (at λ~1)	74-77	12-15	0.05-0.5	0.1-2	3-10
diesel motor	76-78	4-10	0.01-0.5	5-18	1-5
Model mixture	90.5	9.5	-	-	-

3. DISCUSSION AND RESULTS

The operating conditions of experimental runs on model mixtures as well as the corresponding CO_2 conversion and CH_4 yield are summarised in Table 2. Runs 1-3 were carried out at constant mass of catalyst (1 g) and GHSV (2 L $h^{-1}g^{-1}$) to compare the performance of the two powder catalyst formulations (Ru 5% dry and Ru 5% Degussa) and the pellet shape. Runs 3-5 were performed with the same catalyst (Ru 0.5% pellet) maintaining constant the total gas flow rate and varying the mass of catalyst (1g, 2g and 3 g) so that GHSV was in the range 0.65 - 2 L $h^{-1}g^{-1}$. Results are reported as CO_2 conversion (X_{CO2}) and CH_4 yield (Y_{CH4}). High selectivity towards CH_4 can be observed in all the runs apart from those with pellets in correspondence of the lowest temperatures, where low conversion of CO_2 was realized. This finding is in line with other works, where high methane selectivity is generally reported with Ru catalysts [10,21,23,26,27].

Table 2 Experimental runs. Other operating conditions are: P = 1 atm; H_2/CO_2 molar ratio = 4

Run	Catalyst	Mass cat. [g]	GHSV [L(STP) h^{-1} g^{-1}]	T [°C]	X_{CO2}	σ_{XCO2}	Y_{CH4}
1	Ru 5% Dry Al_2O_3	1	2	280	0.97	0.03	0.98
				300	0.96	0.07	1.00
				320	0.92	0.05	0.94
2	Ru 5% Degussa	1	2	260	0.51	0.20	0.52
				280	0.69	0.17	0.66
				300	0.60	0.22	0.58
				320	0.59	0.17	0.58
				350	0.46	0.13	0.45
3	Ru 0.5% pellet	1	2	200	0.27	0.1	0.13
				250	0.31	0.06	0.23
				300	0.49	0.12	0.31

				350	0.77	0.06	0.73
4	Ru 0.5% pellet	2	1	200	0.33	0.11	0.11
				250	0.51	0.10	0.34
				300	0.80	0.06	0.72
				350	0.89	0.07	0.83
5	Ru 0.5% pellet	3	0.65	200	0.50	0.14	0.48
				250	0.79	0.07	0.80
				300	0.92	0.06	0.87
				350	0.85	0.05	0.81

The curves of CO_2 conversion for all the runs performed are reported in Fig. 1.

As can be observed, the formulation of the catalyst, the temperature and the GHSV all played a role in determining the value of the CO_2 conversion. However, above 260 °C, the CO_2 conversion was always > 50% except for run 3 where the pellet catalyst was tested with the highest space velocity (i.e. the lowest contact time).

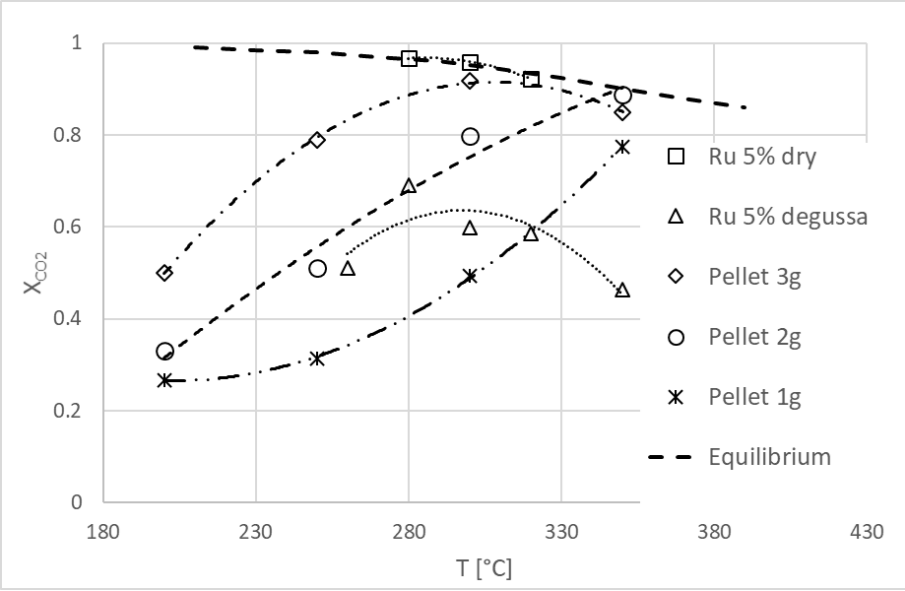

Figure 1 CO_2 conversion in function of temperature for all runs

The CH_4 yield, depicted in Fig. 2, followed a trend similar to the CO_2 conversion, due to the high selectivity generally observed except for runs 3. The behaviour of the pellet catalyst in the highest GHSV condition can be explained by the very low amount of ruthenium, 10 times less than the other two catalysts.

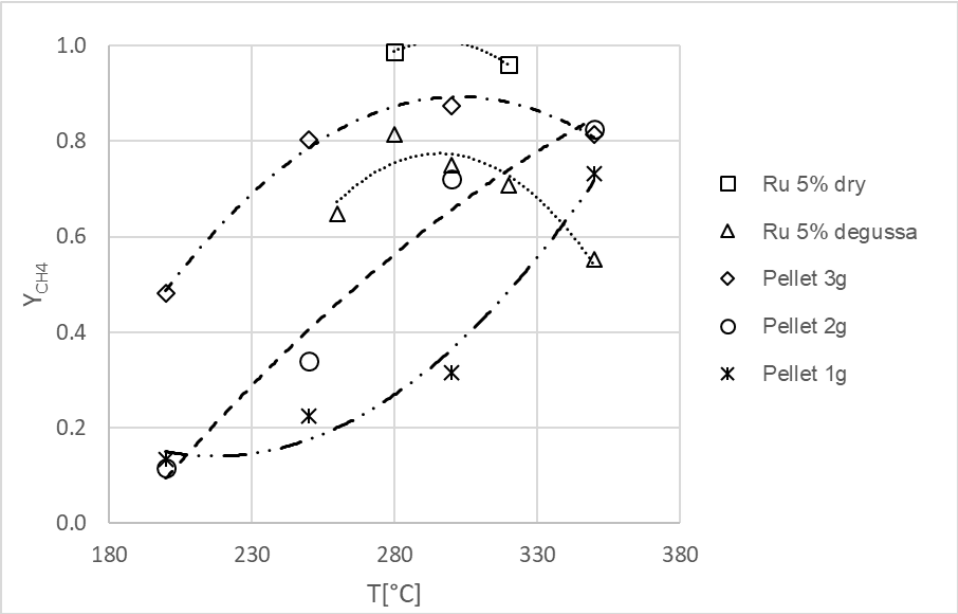

Figure 2 CH_4 yield in function of temperature for all runs

For this reason, the CO_2 conversion at temperatures up to 280-300 °C resulted largely decreased with respect to the other runs. Then, the increasing kinetics favours the achievement of a conversion similar to other runs that are close to the thermodynamic equilibrium. It is interesting to notice the trend of the Ru 5% Degussa, which is characterized by a decrease of the CO_2 conversion after 300 °C, meaning the possible occurrence of deactivation phenomena.

To better highlight the effect of the catalysts' formulation, only the data of runs 1-2-3 are reported in Figure 3.

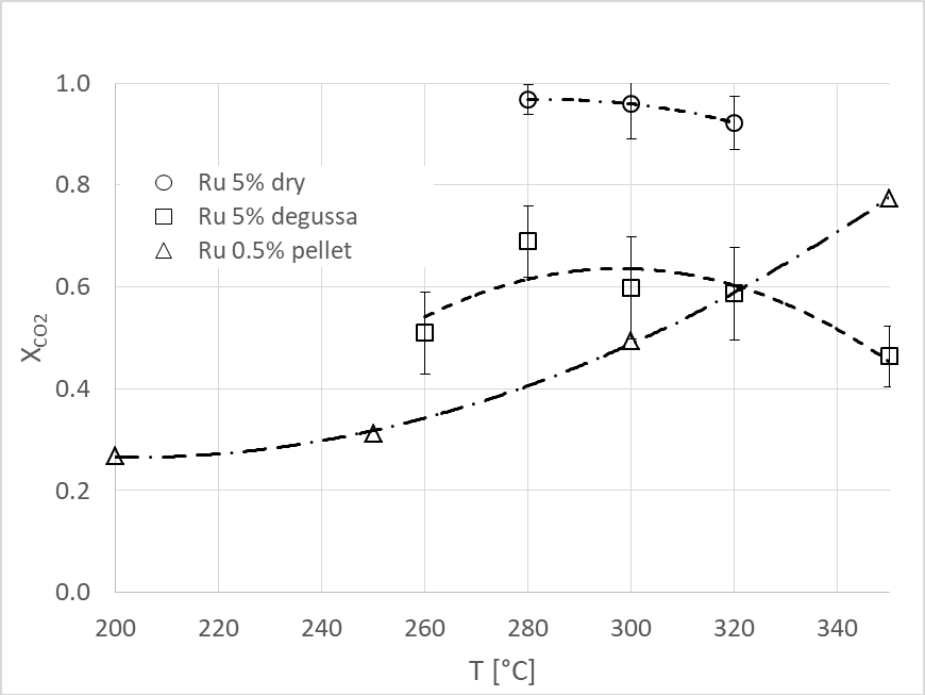

Figure 3 CO_2 conversion at GHSV = 2 $Lh^{-1}g^{-1}$ for the three catalysts

In this case, the GHSV is constant (2 L $h^{-1}g^{-1}$) in the three runs, the only difference being the catalyst. Significant differences can be observed. The curve of CO_2 conversion of the powder catalysts (Ru 5% dry and Ru 5% Degussa) are very similar to those reported by other authors [10,21,23,26,27]. A maximum of CO_2 conversion is observed at 280 – 300 °C. The Ru 5% dry catalyst performs very well, being very close to the thermodynamic limit. However, the conversion obtained with Ru 5% Degussa is quite lower than that with Ru 5% dry, and after a maximum at 300 °C the conversion declines instead of growing towards the TD equilibrium as would be expected because of the increase of temperature and, thus, kinetics. When the catalyst pellet is adopted with the same GHSV value of 2 L $h^{-1}g^{-1}$, the CO_2 conversion for $T \leq 320$ °C is lower with respect to that obtained with powder catalysts and the trend is quite different, even if the maximum value of X_{CO2} reached is very close to the others, being 0.77 observed at T = 350 °C. The described behaviour of these catalysts was correlated to their physico-chemical properties. The active phase in the catalytic conversion of CO_2 to CH_4 is metallic ruthenium [9,10,14,22–26]. Although the catalysts were supplied by Aldrich as alumina supported Ru(0), the phase composition was analyzed by

means of X-ray powder diffraction, being the XRD patterns of the commercial catalysts reported in Fig. 4.

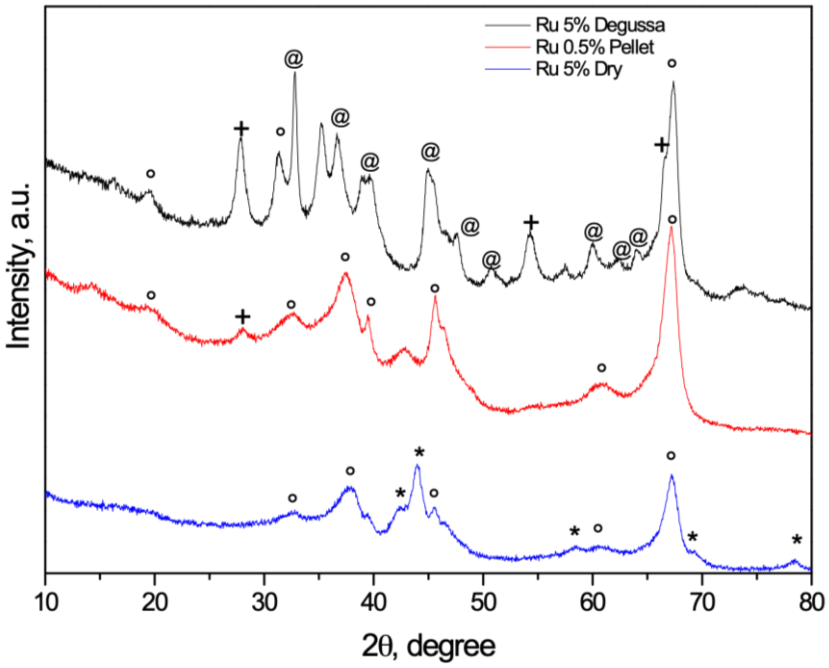

Figure 4 Powders XRD patterns of the commercial catalysts

(o γ- Al_2O_3, JCPDS card No. 10-425; * Ru, JCPDS card No. 6-663; + RuO_2, JCPDS card No. 40-1290; @ Al_2O_3, JCPDS card No. 35-121

The Ru(0) was clearly detected only in sample Ru 5% Dry along with γ-Al_2O_3. On the other hand, mixed alumina phases can be seen in Ru 5% Degussa whereas Ru is present as ruthenium oxide, RuO_2. The very low ruthenium content in the pellet sample (0.5 wt%) could make the ruthenium hardly detectable, however a small peak ascribable to RuO_2 is shown. The ruthenium oxide species may be reduced during the reaction keeping the catalysts active in some extent, considered as negligible the initial amount of metallic ruthenium. To get a greater insight into the Ru/RuO_2 fraction in the three commercial catalysts, the reducibility of the samples was studied by means of the TPR technique.

The TPR profiles of the 5% Degussa, illustrated in fig. 5, revealed a sharp reduction peak at 187 °C with a shoulder at lower temperature.

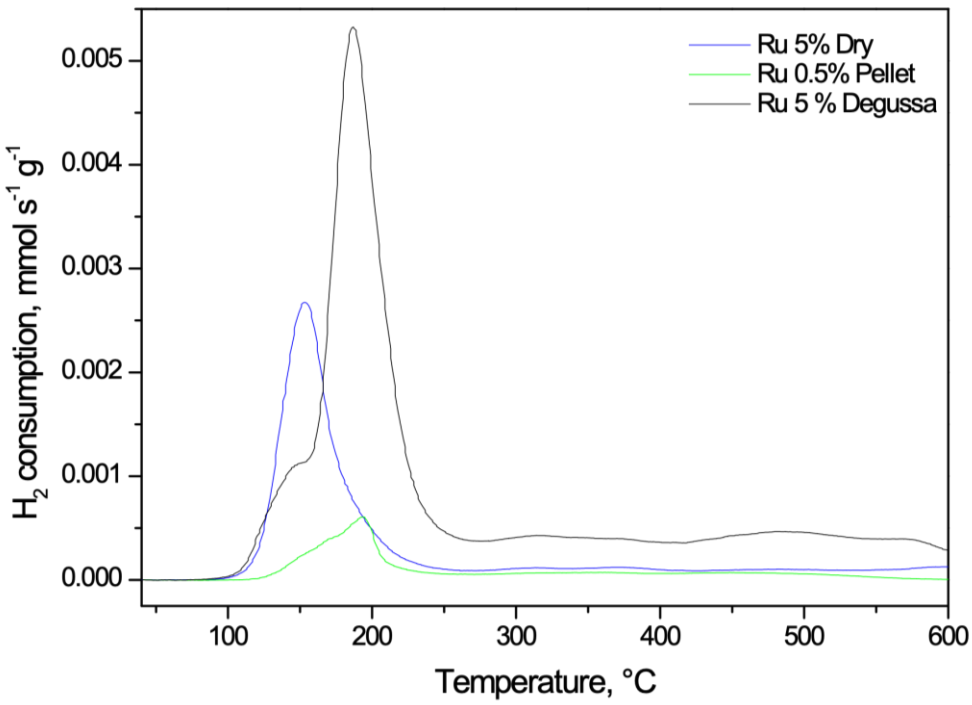

Figure 5 TPR spectra of commercial catalysts

The former can be assigned to the one step reduction of Ru^{4+} in a finely dispersed RuO_x species [28,29], and the latter is likely to be related to the reduction of Ru^{3+} either formed by the partial oxidation of superficial Ru or by the not complete decomposition of the Ru precursor [28–30]. The peak at 153 °C is the only peak displayed be the catalyst Ru 5% Dry. The overall H_2 consumption (241 μmol g^{-1} for Ru 5% Degussa and 119 μmol g^{-1} for Ru 5% Dry) revealed that the reducible ruthenium fraction is nearly double in the sample Ru 5% Degussa, meaning a double amount of ruthenium in the oxidized state. These findings are in agreement with the XRD results. The catalyst Ru 0.5 % pellet showed one reduction peak; however, the asymmetric profile of the peak indicates the presence of at least two components, resembling the spectra of the Ru 5% Degussa. Finally, a hydrogen consumption of 27 μmol g^{-1} is consistent with a ruthenium content 10 times lower. A phenomenon of spillover occurring on the formed Ru(0) particles can account for the further H_2 consumption above 300 °C [28,31].

The textural characteristics of the as-purchased catalysts were evaluated by the analysis of the corresponding N_2 adsorption isotherms at -196 °C (not reported). All catalysts possessed inter-particles mesopores and showed comparable surface area, as reported in Table 3.

Table 3. Samples properties as derived from N_2 sorption isotherms at -196°C

Sample	S_{BET} ($m^2\ g^{-1}$)	Total Pore Volume ($cm^3\ g^{-1}$)	Micropore Volume ($cm^3\ g^{-1}$)	Pore Diameter (nm)[a]
Ru 5% Dry	97	0.27	/	5-15
Ru 5% Degussa	108	0.42	/	8-25
Ru 0.5% Pellet	109	0.26		4-20

[a]As obtained by applying the NL-DFT method

On the other hand, pore diameter shifted to higher values in the case of Ru 5% Degussa. From these results, it can be concluded that the catalytic performance was significantly affected by the content of active phase and its oxidation state. When metallic Ru is considerably present on the surface, the conversion is very close to the thermodynamic limit, whereas when ruthenium is in the form of oxide the conversion is strongly limited and a reducing pre-treatment has to be considered.

Additionally, a possible reason to explain the trend of the catalyst in pellet could be the limited mass of pellets loaded (1 g) and the higher fraction of void with respect to powder catalysts, the contact time is lower than the time necessary to the methanation reaction. At higher temperature (T = 350 °C), the time necessary to the reaction diminishes and can even become lower than the already short contact time due to the limited amount of catalyst.

The results of runs 3-5, obtained using Ru pellets, are compared in Fig. 6 to show the effect of GSHV on the CO_2 conversion as a function of the temperature. It is interesting to observe how the curves of

conversion change when GHSV vary from 0.65 to 2 L $h^{-1}g^{-1}$. With the lowest GHSV, meaning the highest amount of catalyst loaded, the behaviour is very similar to that of catalyst Ru 5% dry powder, as reported in Fig. 1.

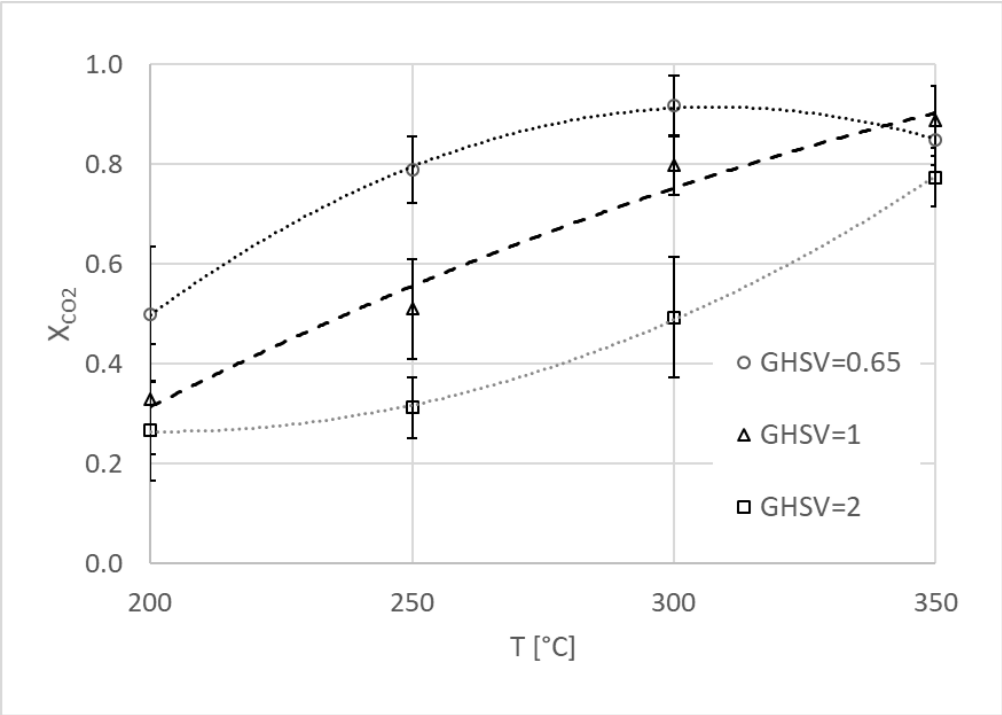

Figure 6 CO_2 Effect of reaction temperature and GHSV on X_{CO2} conversion using pellets Ru 0.5%.

Fig. 7 shows how the CO_2 conversion changes with GHSV. In fact, if GHSV = 0.65 L $h^{-1}g^{-1}$ a temperature of 250 °C was enough to reach $X_{CO2} \approx 0.8$ and the maximum conversion was reached at 300 °C (X_{CO2} = 0.92). If the mass of catalyst was reduced so that GHSV = 1 L $h^{-1}g^{-1}$, a temperature of 300 °C was necessary to obtain $X_{CO2} > 0.8$ and the maximum conversion was reached at 350 °C with $X_{CO2} = 0.89$. The effect of temperature is still more evident when the mass of catalyst was at its minimum. In this case, GHSV = 2 L $h^{-1}g^{-1}$ and it was necessary to reach a temperature of 350 °C to have a conversion of CO_2 $X_{CO2} = 0.77$. So, the CO_2 conversion reduces with GHSV at all temperatures investigated. At T=350 °C the reduction was more limited. Similar finding has been observed both at 310 and 290 °C on Ru powder catalyst in the range GHSV 3.75-10 L (STP)$h^{-1}g^{-1}$ by [10].

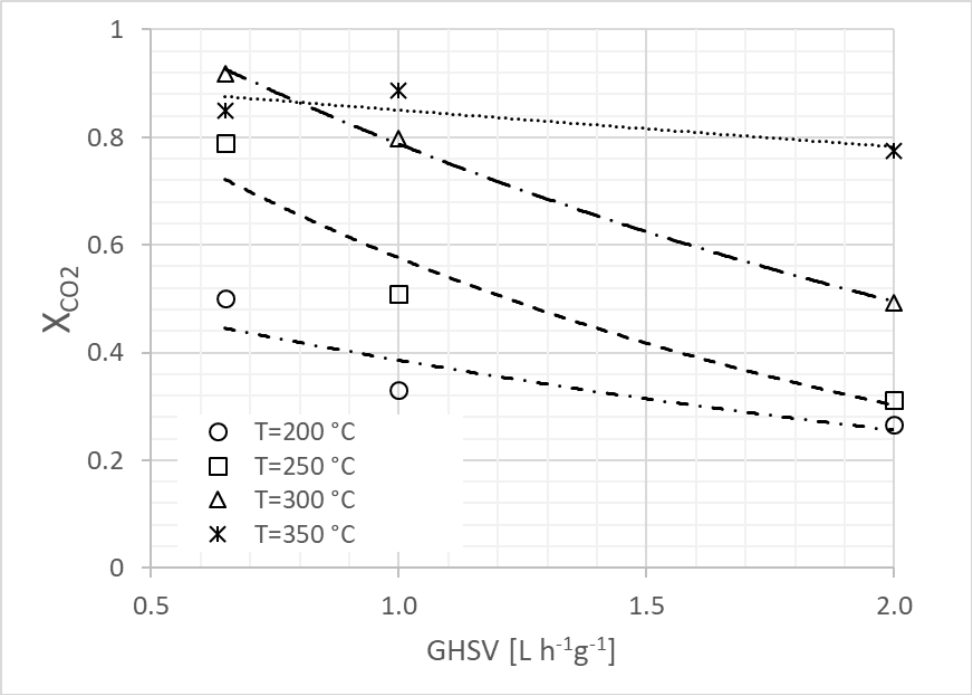

Figure 7 Effect of GHSV on X_{CO2} at different temperatures. Pellets Ru 0.5%.

The results obtained with pellets at GHSV = 0.65 L $h^{-1}g^{-1}$ are of great interest, being very similar to those with Ru 5% dry powder at GHSV= 2 L $h^{-1}g^{-1}$ (see Fig. 1). In fact, they indicate that the mass transfer resistance due to diffusion inside the porosity of the catalyst was not negligible but was limited and did not influence deeply the rate of the methanation process. According to Falbo et al. [10], it was supposed that a non-uniform distribution of the active metal on the pellet occurred. This was confirmed by the FESEM analysis, whose cross-section micrograph of the sample with the average content of ruthenium in different areas is illustrated in Fig. 8. The micrograph shows the portion from the centre of the pellet to its outer edge. As can be appreciated, an eggshell distribution of the active phase was present, with the complete absence of Ru in the core, a nominal content of 0.5 wt% of Ru in the central shell between the core and the edge and a higher Ru content (1.5 wt%) in the outer shell of the pellet, whose thickness was estimated to be 100-150 μm. This value is only slight larger than average powder diameter (45-75 μm).

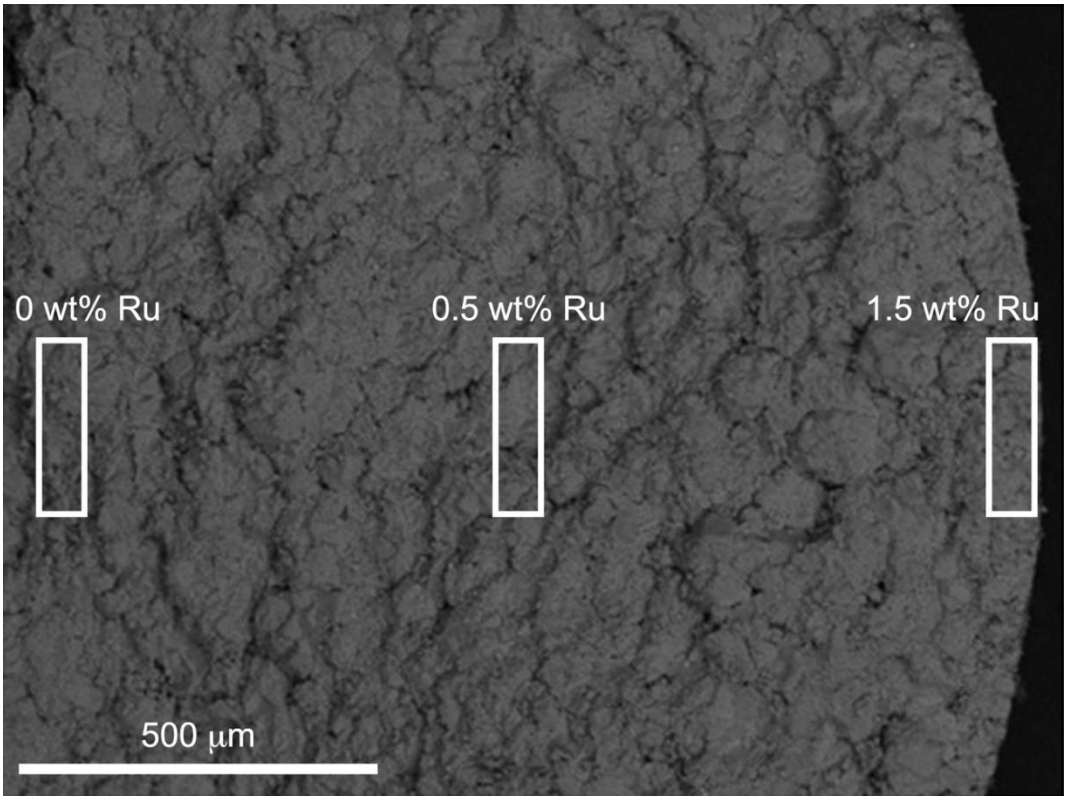

Figure 8 Cross-section fracture micrograph of the pellet catalyst (from the centre to the outer edge), reporting average Ru content in different areas

A triple loading of catalyst as in run 5 leads to a total amount of active metal interested in the catalytic process that is almost the same of the Ru 5% dry catalyst.

The results obtained were free of external or convective mass transfer limitations. In fact, the absence of external mass transfer limitations has been theoretically checked and this was confirmed by the tests reported in Falbo et al. [10], using an experimental apparatus like our but at a less linear gas velocity. In fact, they used a similar but larger reactor (internal diameter 1.1 cm vs 0.8 cm in this study), a higher GHSV (3.75-7.50 L $h^{-1}g^{-1}$) and a lower mass of catalyst (0.375 g). From this data, it is possible to evaluate the empty column linear velocity at STP. In our tests, it was constant and equal to 1.1 cm s^{-1}, while in the tests carried out by Falbo et al. [10] it ranged between 0.4 and 0.8 cm s^{-1}. Therefore, linear velocity, which mass transfer resistance depends on, in our operating conditions was higher than that used by Falbo et al. [10].

Development of methanation reactors. The results obtained with pellets confirm the real possibility to use Ru catalysts to reduce CO_2 emissions at vehicle exhausts [21]. In fact, with pellets pressure drops are at a minimum and back pressure does not influence engine efficiency. Based on the results obtained, it is possible to size the methanation reactor. We have considered a gasoline and a diesel vehicle respectively of 1300 and 2100 cc of cylinder capacity. In both cases a regime rpm is assumed, and flow rate exhaust is calculated ($Q_g = 2.4 \cdot 10^4$ L h^{-1} for the gasoline vehicle and $Q_d = 7{,}6 \cdot 10^4$ L h^{-1}). To size the methanation reactor we make the hypothesis that 10% of whole exhaust flow is treated and assume GHSV = 0.65 L $h^{-1} g^{-1}$ to have a higher CO_2 conversion. The volume of the methanation is $V_g = 2.3$ L for the gasoline vehicle while $V_d = 7.2$ L for the diesel vehicle. The corresponding mass of the reactor would be about 4 and 12 kg respectively in the two cases. Both volume and mass do not represent a significant inhibition to real application. The size of the methanation reactor depends mainly from the GHSV value. Our calculation was conservative by employing a quite low value of GHSV (0.65 L h-1 g-1). In the literature, high CO_2 conversion and methane yield are reported with GHSV 10-30 times higher than ours [32]. Therefore, the possibility to convert up to 20-30% of CO_2 would be not unfeasible, resulting in a significant decrease of the CO_2 emission in the face of potential costs due to the increased technological complexity.

In automotive after-treatment catalytic applications as three-way catalytic converters, lean NO_x traps, selective catalytic reduction (SCR) reactors [33] thin-wall and high cell density substrates are used to improve contacting efficiency between the exhaust gas and the active catalyst, and to lower the thermal mass of the converter [34]. These structures are named monolithic reactors. Several materials are used as supports: alumina, silica or silicon carbide. Diesel particulate filters (DPFs) have also a similar structure with the difference that they are wall-flow devices besides of flow-through devices as catalytic converters are, thus with higher pressure drops.

The experimental results obtained with pellets and the characterization analysis of the distribution of the active metal (Fig. 8) indicate that, in order to obtain a high conversion, it is enough a Ru content of 1.5 wt% in the outer surface for a depth of about 500 μm. Typical values of the thickness of ceramic supports of monolithic reactors are in the range .05÷0.10 mm. In this way, the catalyst effectiveness is maximized.

Due to the high specific surface of the channels the size of the monolithic reactor will be less than that of the pellet fixed bed reactor above evaluated. The CH_4 produced in the methanation reactor would be recirculated into the intake manifold, using technologies already developed for EGR (exhaust gas recirculation) used to control NO_x emissions [30].

The CH_4 produced in the methanation reactor would be recirculated into the intake manifold, using technologies widely applied on today automobile engines to reduce NO_x formation [35], like the exhaust gas recirculation system (EGR), as already reported in [21]. The EGR technique was firstly adopted in diesel engines and finds application in all diesel engines, from light-duty to heavy-duty engines and also to low-speed two-stroke marine engines. At present, owing to the growing energy and environment problems, EGR is also commonly used in gasoline engines. The percentage of the recirculated exhaust gas depends on the various working modes of the engine, ranging from 20-30% in gasoline engines and up to 50% in diesel engines [35].

Finally, the temperature control of the methanation reactor could be easily achieved using the temperature control system of the vehicle. Ambient air and exhaust gas could be tuned to cool or heat the reactor as necessary.

One of the main technological restriction for the industrial development of the methanation process at vehicle exhausts is the need of hydrogen on board. However, some solutions are at an advanced stage of development: i) hydrogen could be stored in cylinders to be refilled at stations at the same time of fuel. The task is less complex with respect to full hydrogen motor vehicles because the hydrogen amount is significantly lower; ii) hydrogen could be stored using materials with high hydrogen storage capacity. Researches in this field are intensive on different kind of materials [36,37]; iii) hydrogen could be produced by water electrolysis with growing efficiency, as reported in recent works [38–40]. Water would be refilled at stations at the same time of fuel.

4. CONCLUSIONS

Two powder and one pellet commercial Ru catalysts with different Ru content have been tested in a methanation experiment. Operating conditions explored are: temperature 200-350 °C; GHSV = 0.65-2 $Lh^{-1}g^{-1}$, H_2/CO_2 ratio = 4; and P = 1 atm. Significant CO_2 conversion differences have been observed between the two powder catalysts with in one case (Ru 5% reduced dry) maximum CO_2 conversion equal to 0.97 and in the other (Ru 5% Degussa) 0.69 both at T = 280 °C. In both cases CH_4 selectivity is very high. The different behavior in the conversion trends are demonstrated to be attributable to the physico-chemical properties, in particular the amount of active phase (ruthenium) and its oxidation state. The performances of the catalyst pellet, containing a nominal Ru amount 10 times lower than the powder catalysts, in the same operating conditions of powder catalysts are generally lower. However, the increase of the loaded amount of catalyst (i.e. to reduce GHSV from 2 to 0.65 L $h^{-1}g^{-1}$) by a factor of three allows to obtain performances similar to the best one of the powder catalysts with CO_2 conversion of 0.92 at T = 300 °C, due to the fact that the superficial content of Ru is higher than the nominal one (1.5 wt%) and, by raising the catalyst loading, the total quantity of ruthenium interested in the reaction is comparable to the one of the most performing powder catalyst (Ru 5% dry). The use of pellets in a fixed bed or of a monolithic reactor guarantees the minimization of the back pressure and the real possibility to apply methanation with Ru catalysts at vehicles exhaust. Based on the results obtained, the volume and mass of the methanation reactor were evaluated. The order of magnitude is 2.5 L of volume and 4 kg of mass of methanation reactor for a 1300 cc gasoline vehicle. The methane produced can be recirculate into the intake manifold, in a similar way to EGR (Exhaust Gas Recirculation) used to control NOx emissions [35].

Main obstacles to the commercial development of the process are: a safe, effective and economic way to store or produce hydrogen on the vehicle, and the individuation of an economic formulation of the catalyst. The paper does not deal with these topics, but several solutions seem to be within reach of the research. In particular, the most promising are: i) storage of hydrogen using several materials [41] with a wide range of gravimetric and volumetric hydrogen storage capacities; ii) Water electrolysis is a mature technology to produce hydrogen and the need of electric power can be satisfied using natural energy sources like solar energy; iii) new formulations of Ni catalysts could be an economic alternative to noble metal catalysts [9].

Acknowledgments

The contributions of Maria Giuseppa Rosa D'Ambrosio in carrying the experiments and of Giuseppe Perretta of National Council of Research (CNR) – Istituto Motori, Naples for the help in GC analysis are gratefully acknowledged.

References

[1] Sabatier P, Senderens JB. New synthesis of methane. CR Acad Sci 134 (1902) 689–91.

[2] Lashof DA, Ahuja DR. Relative contributions of greenhouse gas emissions to global warming. Nature 344 (1990) 529–531. doi:10.1038/344529a0.

[3] Rego de Vasconcelos B, Lavoie J-M. Recent Advances in Power-to-X Technology for the Production of Fuels and Chemicals. Front Chem 2019;7. doi:10.3389/fchem.2019.00392.

[4] Quintella CM, Hatimondi SA, Musse APS, Miyazaki SF, Cerqueira GS, De Araujo Moreira A. CO_2 capture technologies: An overview with technology assessment based on patents and articles. Energy Procedia, 2011. doi:10.1016/j.egypro.2011.02.087.

[5] Coppola A, Allocca M, Montagnaro F, Scala F, Salatino P. The effect of steam on CO2 uptake and sorbent attrition in fluidised bed calcium looping: The influence of process conditions and sorbent properties. Sep Purif Technol 189 (2017) 101–107. doi:10.1016/J.SEPPUR.2017.08.001.

[6] Centi G, Perathoner S. Opportunities and prospects in the chemical recycling of carbon dioxide to fuels. Catal Today 148 (2009) 191–205. doi:10.1016/J.CATTOD.2009.07.075.

[7] Sakakura T, Choi J-C, Yasuda H. Transformation of Carbon Dioxide. Chem Rev 107 (2007) 2365–2387. doi:10.1021/cr068357u.

[8] Wei W, Jinlong G. Methanation of carbon dioxide: an overview. Front Chem Sci Eng 5 (2011) 2–10. doi:10.1007/s11705-010-0528-3.

[9] Frontera P, Macario A, Ferraro M, Antonucci P. Supported Catalysts for CO2 Methanation: A Review. Catalysts 7 (2017) 59. doi:10.3390/catal7020059.

[10] Falbo L, Martinelli M, Visconti CG, Lietti L, Bassano C, Deiana P. Kinetics of CO2 methanation on a Ru-based catalyst at process conditions relevant for Power-to-Gas applications. Appl Catal B Environ 225 (2018) 354–363. doi:10.1016/J.APCATB.2017.11.066.

[11] Champon I, Bengaouer A, Chaise A, Thomas S, Roger A-C. Carbon dioxide methanation kinetic

model on a commercial Ni/Al_2O_3 catalyst. J CO_2 Util 34 (2019) 256–265. doi:10.1016/J.JCOU.2019.05.030.

[12] Aresta M, Nocito F, Di Benedetto A. What Catalysis Can Do for Boosting CO_2 Utilization. Adv Catal 62 (2018) 49–111. doi:10.1016/BS.ACAT.2018.08.002.

[13] Alarcón A, Guilera J, Díaz JA, Andreu T. Optimization of nickel and ceria catalyst content for synthetic natural gas production through CO2 methanation. Fuel Process Technol 193 (2019) 114–22. doi:10.1016/J.FUPROC.2019.05.008.

[14] Sharma S, Hu Z, Zhang P, McFarland EW, Metiu H. CO2 methanation on Ru-doped ceria. J Catal 278 (2011) 297–309. doi:10.1016/J.JCAT.2010.12.015.

[15] Pan Q, Peng J, Sun T, Gao D, Wang S, Wang S. CO2 methanation on Ni/Ce0.5Zr0.5O2 catalysts for the production of synthetic natural gas. Fuel Process Technol 123 (2014) 166–171. doi:10.1016/J.FUPROC.2014.01.004.

[16] Abate S, Mebrahtu C, Giglio E, Deorsola F, Bensaid S, Perathoner S, et al. Catalytic Performance of γ-Al_2O_3–ZrO_2–TiO_2–CeO_2 Composite Oxide Supported Ni-Based Catalysts for CO_2 Methanation. Ind Eng Chem Res 55 (2016) 4451-4460. doi:10.1021/acs.iecr.6b00134.

[17] Abate S, Barbera K, Giglio E, Deorsola F, Bensaid S, Perathoner S, et al. Synthesis, Characterization, and Activity Pattern of Ni-Al Hydrotalcite Catalysts in CO_2 Methanation. Ind Eng Chem Res 55 (2016) 8299-8308. doi:10.1021/acs.iecr.6b01581.

[18] Giglio E, Deorsola FA, Gruber M, Harth SR, Morosanu EA, Trimis D, et al. Power-to-Gas through High Temperature Electrolysis and Carbon Dioxide Methanation: Reactor Design and Process Modeling. Ind Eng Chem Res 57 (2018) 4007-4018. doi:10.1021/acs.iecr.8b00477.

[19] European Environment Agency (EEA). Focusing on environmental pressures from long distance transport. TERM 2014: transport indicators tracking progress towards environmental targets in Europe. 2014.

[20] European Union (2019) Regulation (UE) No 2019/631 of 17 April 2019. setting CO2 emission performance standards for new passenger cars and for new light commercial vehicles, and repealing Regulations (EC) No 443/2009 and (EU) No 510/2011. Off J Eur Union 2019; L111:13–53.

[21] Murena F, Prati M V. Catalytic Conversion of CO_2 to CH_4 with a Ru Catalyst: Application at Vehicle Exhaust. Emiss Control Sci Technol 3 (2017) 220–229. doi:10.1007/s40825-017-0067-1.

[22] Brooks KP, Hu J, Zhu H, Kee RJ. Methanation of carbon dioxide by hydrogen reduction using the Sabatier process in microchannel reactors. Chem Eng Sci 62 (2007) 1161–70. doi:10.1016/J.CES.2006.11.020.

[23] Zağli E, Falconer JL. Carbon dioxide adsorption and methanation on ruthenium. J Catal 69 (1981) 1–8. doi:10.1016/0021-9517(81)90122-6.

[24] Wang W, Wang S, Ma X, Gong J. Recent advances in catalytic hydrogenation of carbon dioxide. Chem Soc Rev 40 (2011) 3703. doi:10.1039/c1cs15008a.

[25] Garbarino G, Bellotti D, Finocchio E, Magistri L, Busca G. Methanation of carbon dioxide on Ru/Al_2O_3: Catalytic activity and infrared study. Catal Today 277 (2016) 21–8. doi:10.1016/J.CATTOD.2015.12.010.

[26] Garbarino G, Bellotti D, Riani P, Magistri L, Busca G. Methanation of carbon dioxide on Ru/Al_2O_3 and Ni/Al_2O_3 catalysts at atmospheric pressure: Catalysts activation, behaviour and stability. Int J Hydrogen Energy 40 (2015) 9171–9182. doi:10.1016/J.IJHYDENE.2015.05.059.

[27] Hwang S, Smith R. Optimum Reactor Design in Methanation Processes with Nonuniform Catalysts. Chem Eng Commun 196 (2008) 616–42. doi:10.1080/00986440802484465.

[28] Esposito S, Silvestri B, Russo V, Bonelli B, Manzoli M, Deorsola FA, et al. Self-Activating Catalyst for Glucose Hydrogenation in the Aqueous Phase under Mild Conditions. ACS Catal 9 (2019) 3426–3436. doi:10.1021/acscatal.8b04710.

[29] Minieri L, Esposito S, Russo V, Bonelli B, Di Serio M, Silvestri B, et al. A Sol-Gel Ruthenium-

Niobium-Silicon Mixed-Oxide Bifunctional Catalyst for the Hydrogenation of Levulinic Acid in the Aqueous Phase. ChemCatChem 9 (2017) 1476–1486. doi:10.1002/cctc.201601547.

[30] Zheng J, Wang C, Chu W, Zhou Y, Köhler K. CO_2 Methanation over Supported Ru/Al_2O_3 Catalysts: Mechanistic Studies by In situ Infrared Spectroscopy. Chemistry Select 1 (2016) 3197–3203. doi:10.1002/slct.201600651.

[31] Esposito S, Dell'Agli G, Marocco A, Bonelli B, Allia P, Tiberto P, et al. Magnetic metal-ceramic nanocomposites obtained from cation-exchanged zeolite by heat treatment in reducing atmosphere. Microporous Mesoporous Mater 268 (2018) 131–43. doi:10.1016/J.MICROMESO.2018.04.024.

[32] Razzaq R, Zhu H, Jiang L, Muhammad U, Li C, Zhang S. Catalytic Methanation of CO and CO 2 in Coke Oven Gas over $Ni–Co/ZrO_2–CeO_2$. Ind Eng Chem Res 52 (2013) 2247–56. doi:10.1021/ie301399z.

[33] Johnson T, Joshi A. Review of Vehicle Engine Efficiency and Emissions. SAE Int J Engines 11 (2018) 2018-01–0329. doi:10.4271/2018-01-0329.

[34] Association (Meca) Manufacturers of Emission Controls. LEV III and Tier 3 Exhaust Emission Control Technologies for Light-Duty Gasoline Vehicles February. Meca White Rep 2015.

[35] Wei H, Zhu T, Shu G, Tan L, Wang Y. Gasoline engine exhaust gas recirculation – A review. Appl Energy 99 (2012) 534–44. doi:10.1016/J.APENERGY.2012.05.011.

[36] Mohan M, Sharma VK, Kumar EA, Gayathri V. Hydrogen storage in carbon materials—A review. Energy Storage 1 (2019) e35. doi:10.1002/est2.35.

[37] Abe JO, Popoola API, Ajenifuja E, Popoola OM. Hydrogen energy, economy and storage: Review and recommendation. Int J Hydrogen Energy 44 (2019) 15072–15086. doi:10.1016/j.ijhydene.2019.04.068.

[38] Hashimoto K, Kumagai N, Izumiya K, Takano H, Kato Z. The production of renewable energy in the form of methane using electrolytic hydrogen generation. Energy Sustain Soc 4 (2014) 17.

doi:10.1186/s13705-014-0017-5.

[39] Chapman A, Itaoka K, Hirose K, Davidson FT, Nagasawa K, Lloyd AC, et al. A review of four case studies assessing the potential for hydrogen penetration of the future energy system. Int J Hydrogen Energy 44 (2019) 6371–6382. doi:10.1016/j.ijhydene.2019.01.168.

[40] Parra D, Valverde L, Pino FJ, Patel MK. A review on the role, cost and value of hydrogen energy systems for deep decarbonisation. Renew Sustain Energy Rev 101 (2019) 279–94. doi:10.1016/j.rser.2018.11.010.

[41] Durbin DJ, Malardier-Jugroot C. Review of hydrogen storage techniques for on board vehicle applications. Int J Hydrogen Energy 38 (2013) 14595–14617. doi:10.1016/J.IJHYDENE.2013.07.058.